

Mössbauer study of the magnetocaloric compound AlFe_2B_2

Johan Cedervall¹ · Lennart Häggström¹  ·
Tore Ericsson¹ · Martin Sahlberg¹

© Springer International Publishing Switzerland 2016

Abstract Mössbauer spectroscopy in the ferromagnetic AlFe_2B_2 reveals $T_c = 299$ K and shows good agreement with magnetic measurements. The crystals are plate-shaped. The flakes are found from X-ray diffraction to be in the crystallographic ac -plane in the orthorhombic system. The axes of the principle electric field gradient tensor are, by symmetry, colinear with the crystal a -, b - and c -axes. By using information about the quadrupole splitting and line asymmetry in the paramagnetic regime together with the quadrupole shift of the resonance lines in the ferromagnetic regime the magnetic hyperfine field direction is found to be in the ab -plane having an angle $\leq 40^\circ$ to the b -axis.

Keywords Mössbauer spectroscopy · Magnetocaloric material

1 Introduction

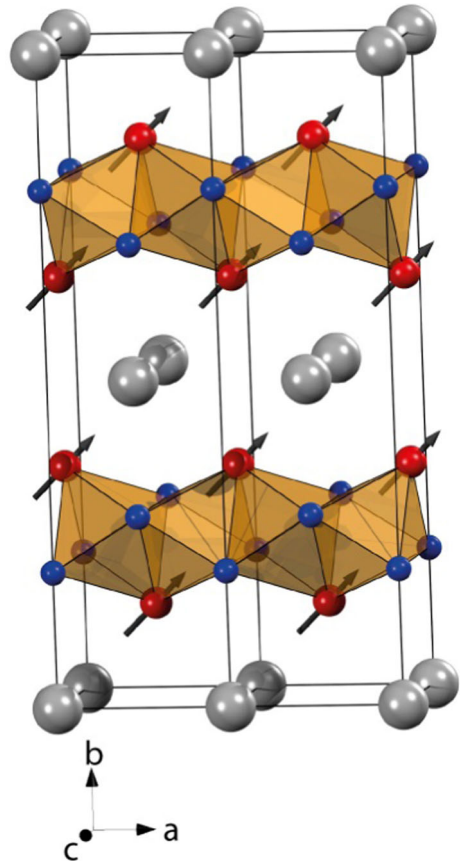
The use of magnetic cooling in refrigerators as a replacement for conventional gas cooling devices could lead to lower power consumption and less hazardous materials in the life cycle of the refrigerator [1]. Recently, a new class of materials based on layered AlM_2B_2 ($M = \text{Fe}, \text{Mn}, \text{Cr}$) was proposed as candidate compounds for magnetocaloric applications [2, 3]. The saturation Fe magnetic moment has been reported to $1.15 \mu_B$ [3] and the entropy change at 5 T, ΔS_m to -7.7 J/K·kg around room temperature in AlFe_2B_2 [4]. AlFe_2B_2 crystallizes in

This article is part of the Topical Collection on *Proceedings of the International Conference on the Applications of the Mössbauer Effect (ICAME 2015), Hamburg, Germany, 13–18 September 2015*

✉ Lennart Häggström
lennart.haggstrom@fysik.uu.se

¹ Department of Chemistry – Ångström Laboratory, Uppsala University, Box 538, SE-75121 Uppsala, Sweden

Fig. 1 The orthorhombic crystal structure of AlFe_2B_2 (*red, blue* and *gray* balls symbolize Fe, B and Al atoms respectively). The Fe_2B_2 polyhedra form semi 2-dimensional layers between 1-dimensional Al-layers. The angle between 3 nearby Fe atoms (nearest neighbour distance 2.73 Å) in the same *ab*-plane is 64.5° . Also shown is the possible direction of the Fe magnetic moments found by this study



an orthorhombic structure and show a layered structure with wavy (Fe_2B_2)-slabs between Al atom layers (Fig. 1).

Here we report a study on the synthesis and magnetic properties of AlFe_2B_2 . Single phase samples were prepared using high-temperature synthesis methods gaining high quality AlFe_2B_2 . Magnetic and crystallographic properties were studied with X-ray powder diffraction, Mössbauer spectroscopy and compared with magnetic measurements.

2 Experimental

The samples were synthesised by arc melting, under argon atmosphere, stoichiometric amounts of iron (Leico Industries, purity 99.995 %, surface oxides were reduced in H_2 -gas.), boron (Wacher-Chemie, purity 99.995 %) and aluminium (Gränges SM, purity 99.999 %). To suppress formation of unwanted phases, FeB was first prepared and then AlFe_2B_2 was produced with an excess of 50 % aluminium [2]. To ensure maximum homogeneity the samples were melted 5 times in total. The samples were crushed and pressed into pellets, placed in evacuated silica tubes, annealed for 14 days at 1173 K and subsequently quenched in cold water. Additional phases (e.g. $\text{Fe}_4\text{Al}_{13}$) were removed by etching the samples in diluted HCl (1:1) for 10 minutes.

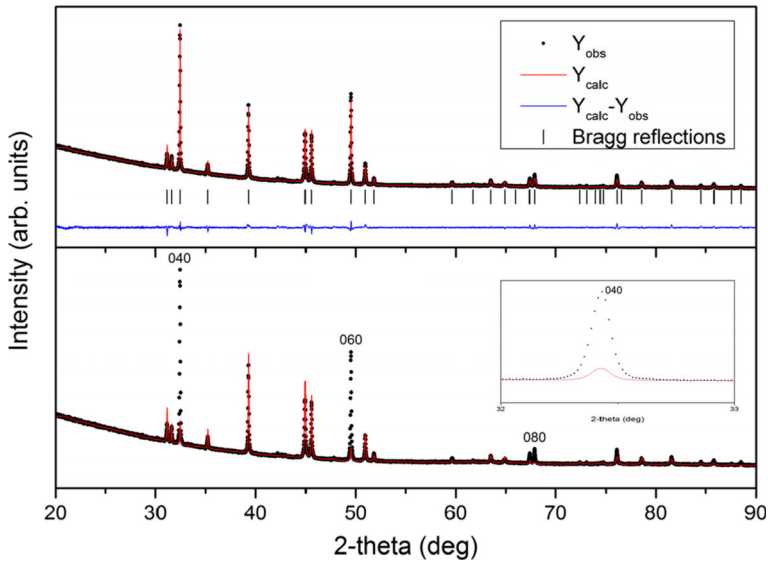


Fig. 2 XRD pattern and refinement with the Rietveld method of the AlFe_2B_2 sample are showed in the upper part of the figure. The texture in the sample is visualised by comparing the observed XRD intensities for the sample (*black dots*) and the calculated powder pattern without texture (*red line*) in the lower part of the figure, the inset shows an enlargement of the 040-peak

X-ray powder diffraction (XRD) intensities were measured using a Bruker D8 diffractometer equipped with a Lynx-eye position sensitive detector (PSD, 4° opening) operating with $\text{CuK}\alpha_1$ radiation ($\lambda = 1.540598 \text{ \AA}$), in a 2Θ range of $20\text{--}90^\circ$. Phase analysis and crystal structure determinations were performed using the Rietveld method [5] implemented in the program Fullprof [6].

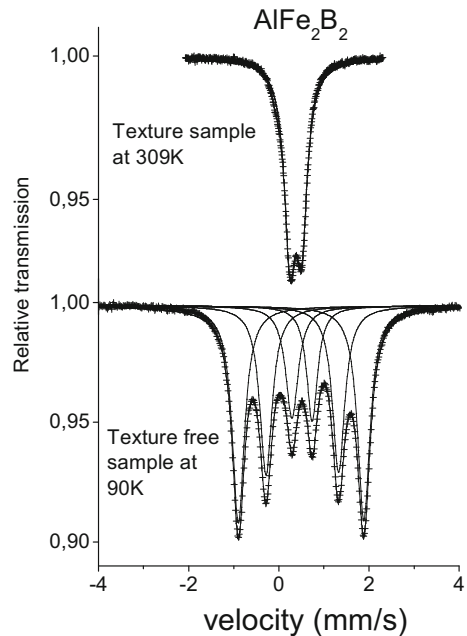
The Mössbauer measurements were carried out, with the absorbers at temperatures between 80 K and 320 K, on a spectrometer with a constant acceleration type of vibrator and a $^{57}\text{CoRh}$ source. Two types of absorbers were prepared. Firstly a slurry of the sample mixed with ethanol was dropped on an thin Al-folie. After ethanol evaporation the flake formed crystallites had sedimented with the flakes parallel to the Al-foil, forming the "textured" absorber I. Another, "texture free" absorber II was made in a loosely packed 1.1 cm^3 cylindrical volume filled with the AlFe_2B_2 powder mixed with boron nitride powder. Calibration spectra were recorded using natural iron foil at room temperature as a reference absorber. Spectra obtained were folded and analysed using a least-squares Mössbauer fitting program.

3 Result and discussion

3.1 X-ray diffraction

The AlFe_2B_2 sample was free of impurities but a high degree of texture (preferred orientation) was observed in the XRD pattern since all $(0\ k\ 0)$ reflections had a significantly higher observed intensity than expected (Fig. 2). This naturally occurring preferred orientation was used to prepare the "textured" absorber I used in the Mössbauer measurements. The unit

Fig. 3 Mössbauer spectra of AlFe_2B_2 at 309 K and at 90 K



cell parameters were determined to be $a = 2.9258(4)$ Å, $b = 11.0278(9)$ Å, $c = 2.8658(3)$ Å, in accordance with previous results [7].

3.2 Mössbauer results in the paramagnetic regime

The Mössbauer spectrum with the γ -ray perpendicular to the “textured” absorber I at 309 K show a slightly resolved asymmetric doublet with $A_+/A_- = 0.92(2)$, $\delta = 0.375(5)$ mm/s, $|\Delta| = 0.259(3)$ mm/s and $\Gamma = 0.250(5)$ mm/s (Fig. 3). A symmetric doublet was observed by El Massalami et al. [2]. Their samples were however hampered by impurities.

The isomer shift, δ , is relative metallic iron at room temperature, $|\Delta|$ is the magnitude of the quadrupole splitting and Γ is the full width at half maximum of the Lorentzians. A_+ (A_-) is the spectral area of the line having the most positive (negative) velocity. The paramagnetic spectrum of the “texture free” absorber II showed a symmetric doublet. A Mössbauer recording using the magic angle of 54.7° [8] between the γ -ray and the normal to the “textured” absorber I gave a symmetric doublet. We can thus conclude that the “texture free” absorber II has no texture while the “textured” absorber I have texture but no Goldanskii-Karyagin (GK) effects. From the X-ray study it is also clear that the flakes in absorber I are predominantly perpendicular to the crystallographic b -axis. The line areas for a doublet of a single crystal, with $A_{3/2}$ being the area of the $3/2 - 1/2$ transition (2 combinations) and $A_{1/2}$ the area of the $1/2 - 1/2$ transition (4 combinations) are given by [9] (thin absorber and no GK effect is assumed):

$$\frac{A_{3/2}}{A_{1/2}} = \frac{4\sqrt{1 + \eta^2/3} + (3\cos^2\alpha - 1 + \eta\sin^2\alpha \cos 2\beta)}{4\sqrt{1 + \eta^2/3} - (3\cos^2\alpha - 1 + \eta\sin^2\alpha \cos 2\beta)}$$

Here α is the polar and β the azimuthal angle for the γ -ray in the principal electric field gradient (EFG) system (Fig. 4). The asymmetry factor of the principle EFG-system is denoted

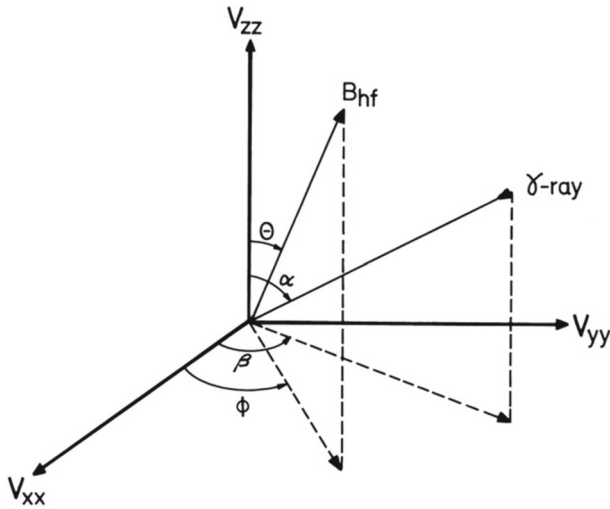


Fig. 4 The principal (xyz) (marked V_{xx} , V_{yy} , V_{zz}) axis of the EFG tensor and the angles involved for the incoming γ -ray and the magnetic hyperfine field B_{hf}

by η . The $3/2 - 1/2$ transition has most positive velocity when $V_{zz} > 0$ and most negative when $V_{zz} < 0$. Fe atoms in the crystal structure are situated in two mirror planes, the ab -plane and the bc -plane. The principal axis (xyz) system of the EFG for the Fe atoms are then coinciding with the crystallographic (abc) system. The orientation of the systems to one another is however undecided.

Because of the flaky nature of $AlFe_2B_2$ we can assume that there is a clear preference for the γ -rays, being normal to the absorber, to be parallel with the crystallographic b -axis. We can therefore restrict ourselves to the cases where the impinging γ -rays are parallel to one of the principal axes of the EFG. The theoretical A_+/A_- -ratio, assuming single crystals, no GK effect and a thin absorber are given in Table 1 below.

As seen from Table 1, our measured value, $A_+/A_- = 0.92(2)$ only fits within one interval, i.e. when $\gamma // V_{xx}$, $V_{zz} > 0$ and $\eta \approx 0.8$. However, our Mössbauer absorber I is not a single crystal, neither a thin absorber. Both these aspects diminish the area contrast in the spectrum, thus A_+/A_- could be smaller than 0.92 in the theoretical case but not larger. In our measurement there is a clear preference for the γ -ray being parallel with the b -axes. The single-crystal character should then be clearly seen in the spectrum, excluding the two other possibilities with area ratio less than 1 (Table 1) i.e. $\gamma // V_{yy}$ and $V_{zz} > 0$, or $\gamma // V_{zz}$ and $V_{zz} < 0$. Accordingly, it is the V_{xx} - axis of the EFG that is parallel with the crystallographic b -axis.

3.3 Mössbauer results in the ferromagnetic regime

The obtained transition temperature between the two magnetic regimes depends slightly on the synthesis routes. For our samples the Curie temperature T_c is found to be 299 K (the Mössbauer spectrum consists then of a superposed paramagnetic doublet and a ferromagnetic sextet with the same intensity) (Fig. 5) The transition region is ± 10 K. Earlier studies have reported T_c in the interval 282 – 320 K [2, 4]. At 90 K the analysis reveal the following hyperfine parameters: $\delta = 0.508(5)$ mm/s, $\varepsilon = -0.012(3)$ mm/s,

Table 1 Theoretical A_+/A_- -ratios for γ being parallel with the three principal EFG axes and different η values

γ -direction	Angles (see Fig. 4)	Assumed signs of V_{zz}	Area ratio	$0 \leq \eta \leq 1$
$\gamma // V_{xx}$	$\alpha = 90^\circ$	$V_{zz} > 0$	$A_+/A_- =$	$0.60 - 1$
	$\beta = 0^\circ$	$V_{zz} < 0$	$A_+/A_- =$	$1.67 - 1$
$\gamma // V_{yy}$	$\alpha = 90^\circ$	$V_{zz} > 0$	$A_+/A_- =$	$0.40 - 0.60$
	$\beta = 90^\circ$	$V_{zz} < 0$	$A_+/A_- =$	$2.50 - 1.67$
$\gamma // V_{zz}$	$\alpha = 0^\circ$	$V_{zz} > 0$	$A_+/A_- =$	$3 - 2.53$
	β undefined	$V_{zz} < 0$	$A_+/A_- =$	$0.33 - 0.40$

$B_{\text{hf}} = 8.75(5)$ T and $\Gamma = 0.253(5)$ mm/s (Fig. 3). Here ε is the electric quadrupole shift and B_{hf} the magnetic hyperfine field. The electric quadrupole shift is defined as $\varepsilon = \frac{eQV_{zz}}{8} \cdot (3\cos^2\theta - 1 + \eta\sin^2\theta\cos 2\phi)$, with the B_{hf} polar and azimuthal angles θ and ϕ , respectively in the principle EFG system (Fig. 4). Q is the nuclear quadrupole moment for the excited $3/2$ -state of ^{57}Fe . El Massalami et al. [2] observed $B_{\text{hf}} = 8.8\text{T}$, while Chai et al. [3] reported $B_{\text{hf}} = 8.87(2)\text{T}$ at 4.2K in good agreement with our findings. Furthermore Chai et al. observed $\varepsilon = -0.02(4)$ mm/s, $\delta = 0.53(2)$ mm/s at 4.2K and also that the Fe magnetic moment was antiparallel to the Fe magnetic hyperfine field B_{hf} .

3.3.1 Analysis of the orientation of B_{hf} versus the crystallographic axes from resonance line positions

In the paramagnetic regime $\Delta = \frac{eQV_{zz}}{2} \cdot \sqrt{1 + \eta^2/3}$. The two values, ε and Δ , are thus related and the parameters θ , ϕ (Fig. 4) and η may be determined, assuming V_{zz} and η being constant over the transition region. The experimental ratio of $\varepsilon/\Delta = -0.046(12)$.

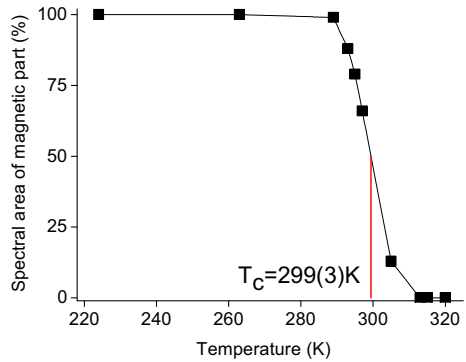
From symmetry point of view one can expect the orientation of B_{hf} to be either along the c -axis or in the ab -plane. If B_{hf} is parallel with the c -axis there are two possibilities for the orientation of the crystal axes versus the EFG principal axes, case 1 and 2 (Table 2). The theoretical ratio ε/Δ for these cases (Table 2) is well outside the experimental value of $-0.046(12)$. Thus we can conclude that B_{hf} is not parallel with the c -axis.

If B_{hf} is oriented in the ab -plane there are also two possibilities for the orientation of the crystal axes versus the EFG principal axes, case 3 and 4 (Table 2). The theoretical and experimental values of ε/Δ are equal within a narrow solution area in the $\eta\theta$ -space for case 3, such that $\theta \approx 58^\circ$ for $\eta = 0$, while $\theta = 90^\circ$ for $\eta \approx 0.8$. Here θ is the angle between B_{hf} and the crystallographic a -axis. For case 4 the theoretical expression for ε/Δ does fit our experimental value, -0.046 , in the interval $(\eta, \phi) = (0.8, 0^\circ)$ to $(1, 38^\circ)$. Here ϕ is the angle between B_{hf} and the crystallographic b -axis. Accordingly, the angle between B_{hf} and the b -axis can be in the interval about 32° to 0° for case 3 and in the interval about 38° to 0° for case 4. Thus, the two possibilities, case 3 and 4, do give roughly the same solutions. We can from this analysis of the hyperfine parameters conclude that the B_{hf} is directed in the ab -plane having an angle to the b -axis between 0° to around 40° .

3.3.2 Analysis of the orientation of B_{hf} versus the crystallographic axes from resonance line areas

Another analysis about the orientation of B_{hf} can be made from the line intensities of the sextets. Here however the thickness effects has to be taken with care. The low temperature

Fig. 5 Experimental spectral area of the magnetic part in the Mössbauer spectra of $AlFe_2B_2$ as a function of temperature. The transition temperature T_c is set where the magnetic and non-magnetic spectral area are the same



spectra of the "texture free" absorber II and the "textured" absorber I were compared. The experimental line intensities of the sextets from the fits are given in Table 3.

For a texture free absorber the theoretical Mössbauer line intensity ratios in the thin absorber limit are 3:2:1. The experimental intensities deviates from these due to thickness effects and from texture persisting in the absorber. To further check any texture in the "texture free" absorber II we performed an analysis program as given by Williams and Brooks [10]. The thin absorber ratio I_1/I_3 would be 3:1 irrespective of any texture. From the tables as presented by Williams and Brooks a experimental ratio $I_1^*/I_3^* = 2.12$ would arise for a effective thickness parameter $t_3 = 1.21$ for line 3 and consequently $t_1 = 3 \cdot 1.21 = 3.63$ for line 1. With the found intensity I_2^* for absorber II the effective thickness parameter for line 2 was calculated, using the area expression for $A(t)$ [10], to $t_2 = 2.40$. Normalizing the found effective thickness parameters gave the thin absorber limit ratio 3:1.98:1 (Table 3). Within error this shows, once more, that absorber II is a texture-free absorber. The thickness effect is stronger for the absorber I as compared to the absorber II as revealed by the much less experimental I_1^*/I_3^* ratio. Using the same analysis for the spectrum of absorber I as for spectrum of absorber II gave the thin absorber limit ratio of 3:1.75:1 for the absorber I (Table 3). The deviation from the ratio 3:2:1 is a clear indication of texture effects. The thin absorber ratios for a texture polarized sample with γ -ray having an angle γ_m to the magnetic hyperfine field B_{hf} is given by $3(1 + \cos^2 \gamma_m) : 4 \sin^2 \gamma_m : (1 + \cos^2 \gamma_m)$ [10]. In the present case the γ -ray direction is parallel with the b -axis. From the found thin absorber ratios 3:1.75:1 the average angle γ_m can be calculated to be $\approx 50^\circ$. The errors involved in this analysis are quite large. The "textured" absorber I is not a full texture polarized absorber but have also randomized structures. The presently calculated value of γ_m is thus an average value for a superposed absorber with random orientation represented by $\gamma_m = 54.7^\circ$ and oriented flakes having $0^\circ < \gamma_m < 40^\circ$ as found above from the hyperfine field analysis (Section 3.3.1)

From a neutron diffraction study recently performed by us but not yet fully analyzed the Fe magnetic moment was found to be $1.4(3) \mu_B$ at 20 K. The orientation of the Fe moment is furthermore found in the ab -plane and likely in a direction pointing towards the nearby Fe atoms.

Taking the saturation magnetic hyperfine field as -8.8 T and the value of the Fe magnetic moment of $1.4 \mu_B$ the ratio $B_{hf}/\mu = -6.3$ T / μ_B . The Fermi contact term B_c , emanating from the s -electron polarization at the Fe nucleus, is the most dominating factor to the magnetic hyperfine field. The contact term for Fe has two contributions, one from the core s -electrons, B_{cc} , and one from the s -valence electrons B_{cv} . Since B_{cc} is proportional to the

Table 2 Possible orientations of B_{hf} versus crystal axes (abc) and EFG principal axes (xyz) versus abc , polar and azimuthal angles and corresponding values for ε/Δ

B_{hf}	(xyz) versus (abc)	Angles	Case	ε/Δ
$B_{\text{hf}} // c$	$y//c$	$\theta = 90^\circ$	1	$-0.25 > \frac{-1-\eta}{4\sqrt{1+\eta^2/3}} > -0.43$
	$z//a$	$\phi = 90^\circ$		
	$y//a$	$\theta = 0^\circ$	2	$0.50 > \frac{2}{4\sqrt{1+\eta^2/3}} > 0.43$
	$z//c$			
B_{hf} in the ab -plane	$y//c$	$\phi = 0^\circ$	3	$0.50 > \frac{3\cos^2\theta-1+\eta\sin^2\theta}{4\sqrt{1+\eta^2/3}} > -0.25$
	$z//a$			
	$y//a$	$\theta = 90^\circ$	4	$0.00 > \frac{-1+\eta\cos 2\phi}{4\sqrt{1+\eta^2/3}} > -0.43$
	$z//c$			

The result, $x // b$, from the paramagnetic regime is used

Table 3 Relative experimental line intensities I_1^* , I_2^* and I_3^* for lines 1&6, 2&5 and 3&4 in the sextet, respectively, in the Mössbauer spectra of absorber I and II at 90 K together with thickness corrected relative line intensities I_1 , I_2 and I_3

Absorber	I_1^*	I_2^*	I_3^*	I_1	I_2	I_3
“textured” absorber I	1.90(7)	1.41(6)	1.00	3.00	1.75	1.00
“texture-free” absorber II	2.12(5)	1.63(4)	1.00	3.00	1.98	1.00

magnetic moment with a proportionally factor of about $-13 \text{ T} / \mu_B$ [11], the contribution B_{val} is positive and about 9 T.

4 Conclusion

From detailed analysis of Mössbauer spectra above and below the Curie temperature $T_c = 299 \text{ K}$, it is found that the principle EFG system has axes colinear with the crystallographic abc -axes and $V_{xx} // b$ -axis. The direction of the Fe magnetic hyperfine field B_{hf} have been determined to be in the ab -plane having an angle of less than 40° to the crystallographic b -axis. The nearest Fe - Fe distance is 2.73 \AA in the ab -plane with a direction having an angle of 32° to the b -axis.

References

- Gschneidner, K.A. Jr., Pecharsky, V.K.: Int. J. Refrig **31**, 945 (2008)
- El Massalami, M., Oliviera, D.da.S., Takeya, H.: J. Magn. Magn. Mater **323**, 2133 (2011)
- Chai, P., Stoian, S.A., Tan, X., Dube, P.A., Shatruk, M.: J. Sol. St. Chem **224**, 50 (2015)
- Tan, X., Chai, P., Thompson, C.M., Shatruk, M.: J. of Am. Chem. Soc **135**, 52 (2013)
- Rietveld, H.M.: J. Appl. Cryst. **2**(Pt. 2), 65 (1969)
- Rodríguez-Carvajal, J.: Physica B: Cond. Matter **192**(1–2), 55 (1993)
- Jeitschko, W.: Acta Cryst. B **25**(1), 163 (1969)
- Ericsson, T., Wäppling, R.: J. de Physique **37**, C6–719 (1976). Colloque
- Zory, P.: Phys. Rev. **140**, A1401 (1965)
- Williams, J.M., Brooks, J.S.: Nucl. Instr. and Meth. **128**, 363 (1975)
- Kamali, S., Högström, L., Sahlberg, M., Wäppling, R.: J. Phys. Condens. Matter **23**, 55301 (2011)